PZT Cantilever for Energy Harvesting and Vibration Sensing

Eric Danson and Dong Sam Ha

Multifunctional Integrated Circuits and Systems (MICS) Group

Bradley Department of Electrical and Computer Engineering

Virginia Tech, Blacksburg, VA 24061, USA

{ecdanson, ha}@vt.edu

Abstract—The proposed two-stage ensemble machine learning model aims to bridge the gap between energy harvesting and vibration sensing applications for lead zirconate titanate (PZT) and similar piezoceramic materials by enabling one device to perform both functions simultaneously. Two PZT cantilever configurations were tested: one without a tip mass for maximum linearity at low frequencies and one with a tip mass for maximum energy output. The highest absolute prediction error on the testing set is 19% and 7%, respectively. While the R² score remained nearly 1, the PZT cantilever with the tip mass showed an 11% lower mean absolute error (MAE) and 38% lower mean squared error (MSE) compared to the PZT without, suggesting that PZT cantilevers in energy harvesting configurations can be used to predict acceleration with acceptable accuracy.

Index Terms—PZT, vibration energy harvesting, vibration sensing, accelerometer, machine learning.

I. Introduction

Lead zirconate titanate (PZT) has been used in devices for sensing mechanical force and for harvesting kinetic energy with separate device configurations optimized for each application in terms of size, power output, resonant frequency, bandwidth, and sensitivity to acceleration [1]-[9]. For example, PZT devices designed for measuring acceleration may be small in size and have a high resonant frequency to achieve a linear response in the lower frequencies, while a PZT device designed for energy harvesting may be comparatively large and have a low resonant frequency to match ambient vibration frequencies in the intended environment. We studied how PZT devices respond to acceleration and whether a single device could simultaneously be used for both energy harvesting and vibration sensing. This paper presents that a PZT cantilever set up for energy harvesting can also accurately predict acceleration through machine learning.

Section II reviews piezoelectric transducers and the machine learning models used. Section III presents the proposed method to predict acceleration. Section IV shows the results and a performance comparison between the PZT cantilever setups. Finally, Section V concludes the paper.

II. BACKGROUND

A. Piezoelectric Transducer

PZT is a commonly used piezoelectric ceramic composition for sensors and actuators due to its strong piezoelectric effect [1]. For example, bending a PZT film induces mechanical stress and generates a voltage across the PZT terminals and vice versa. The bidirectional capability to act as a sensor or as an actuator is what makes a PZT device a transducer. Piezoelectric transducers have applications in acoustic sensors as microphones [10], in acoustic actuators as speakers [11], and in energy harvesting by converting vibrations or kinetic energy in the environment to electrical energy [12].

B. Machine Learning Models Used

Machine learning approaches include classification and regression modeling. Classification models predict discrete classes, whereas regression models predict continuous quantities. The models used in this paper are multi-layer perceptron (MLP), extra trees, and support vector regressors. The MLP model is a feedforward neural network comprising input, output, and inner "hidden" layers of artificial neurons [13]. The extra trees model combines multiple decision tree models, each constructed from a random subset of the training data, with random node splitting for each feature [14]. The support vector model uses a kernel function to map features into a higher dimensional space and then finds a hyperplane that maximally separates the data [15].

III. PROPOSED METHOD

A. System Overview

A block diagram for applications using a PZT device for both energy harvesting and vibration sensing is shown in Fig. 1. The power management circuit (PMC) manages the power delivered to the load, and a microcontroller unit (MCU) or field-programmable gate array (FPGA) implements a machine learning model to predict acceleration. This work focuses on the machine learning model.

B. Machine Learning Model

The machine learning model (Fig. 2) is based on a supervised learning approach with an accelerometer's output converted to acceleration in g as the target. The predictors are the PZT output voltage amplitude and frequency. A two-stage ensemble improves the accuracy over that of a single model by combining the outputs of several different models. The first stage comprises three parallel models to provide diversity: MLP, extra trees, and support vector regressors, whose outputs are the input to a single extra trees regressor in the second stage to calculate the final predicted acceleration.

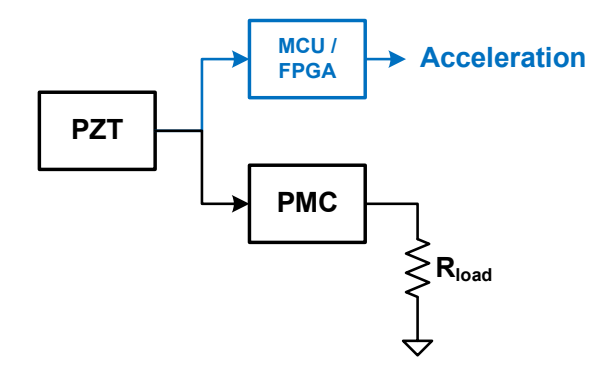


Fig. 1. System overview block diagram.

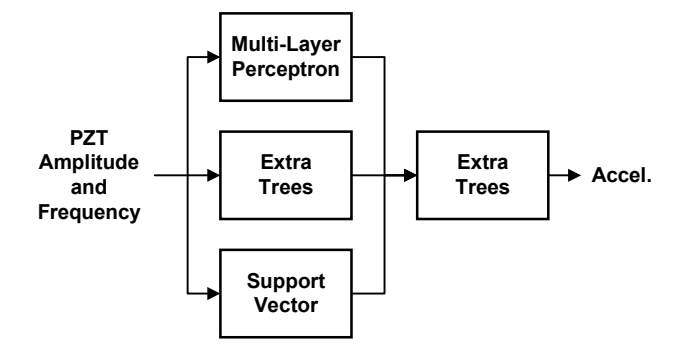


Fig. 2. Machine learning model block diagram.

IV. RESULTS AND DISCUSSION

A. Experiment Setup

The data was collected using an analog ± 8 g microelectromechanical systems (MEMS) accelerometer (Analog Devices ADXL354) and a PZT cantilever (Mide S118-J1SS-1808YB) mounted on a modal shaker (The Modal Shop K2007E01) at constant ambient temperature (Fig. 3). 3Dprinted braces fixed the accelerometer and PZT cantilever to the shaker platform to keep the devices from coming loose during testing, to minimize variance between samples, and to minimize any resonance extrinsic to the devices. Measurement probes and wires were mounted above the shaker platform to avoid weighing down or unbalancing the shaker. The vibration is along the z-axis and parallel to the force of gravity, and the PZT cantilever setup used is effective in only one direction, so only the accelerometer's z-axis output was measured and used as a reference for modeling. The general form of a sinusoid to represent position is

$$x(t) = A\sin(\omega t + \phi),\tag{1}$$

and acceleration is the second derivative of position

$$\frac{\partial^2 x}{\partial t^2} = -A\omega^2 \sin(\omega t + \phi),\tag{2}$$

so a quadratic relationship between acceleration and frequency was expected.

The accelerometer and PZT cantilever output voltages were recorded while sweeping the shaker frequency from 5–200 Hz



Fig. 3. Shaker platform with the accelerometer and PZT cantilever mounted.

at a fixed sinusoidal input amplitude between 25–250 mV in 25 mV increments and with the shaker gain set to 10 dB to cover the reference accelerometer's full operating range. The experiment was successively repeated three times each, with and without mass attachments, specifically magnets, at the end of the PZT cantilever, to ensure repeatability and to observe how the machine learning model performance changes with the PZT configuration. The setup with the tip mass represents the case for maximum energy due to the higher PZT deflection and higher output voltage, and the setup without the tip mass was expected to be more linear at low frequencies due to the higher PZT resonant frequency.

B. Measurement Results

The accelerometer frequency response was converted to acceleration in g using a two-point calibration and shows an approximately linear increase in magnitude with frequency up to 50 Hz at five different amplitudes before saturating (Fig. 4). The shaker displacement decreased with frequency, so the response deviates from the theoretical quadratic relationship in (2) assuming constant displacement. The saturation at higher frequencies is likely due to the shaker behavior because the saturation occurs at all the input amplitudes tested.

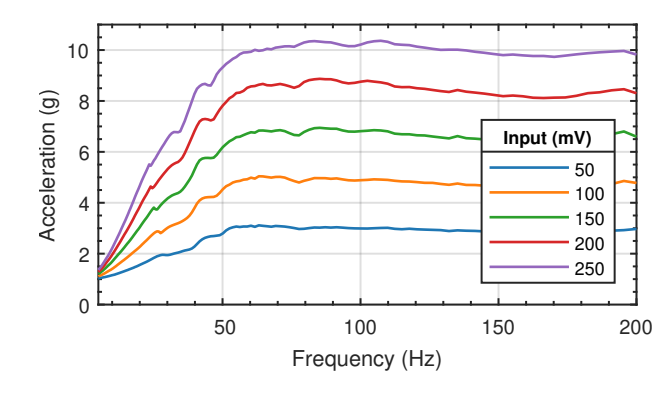


Fig. 4. Accelerometer magnitude from 5-200 Hz.

The PZT cantilever frequency response exhibits a primary resonant peak whose magnitude and frequency depends on the PZT configuration. The PZT cantilever without the tip mass has a resonant peak around 80 Hz (Fig. 5(a)), decreasing to around 20 Hz with the tip mass (Fig. 5(b)). Another resonant peak appears around 30 Hz, possibly due to the measurement probes and wires not being mounted securely and thus systematically interfacing with the shaker platform during measurement. The PZT cantilever without the tip mass is more linear up to 30 Hz with acceleration, while the tip mass increases the PZT output voltage amplitude up to 35 V and hence the amount of energy harvested.

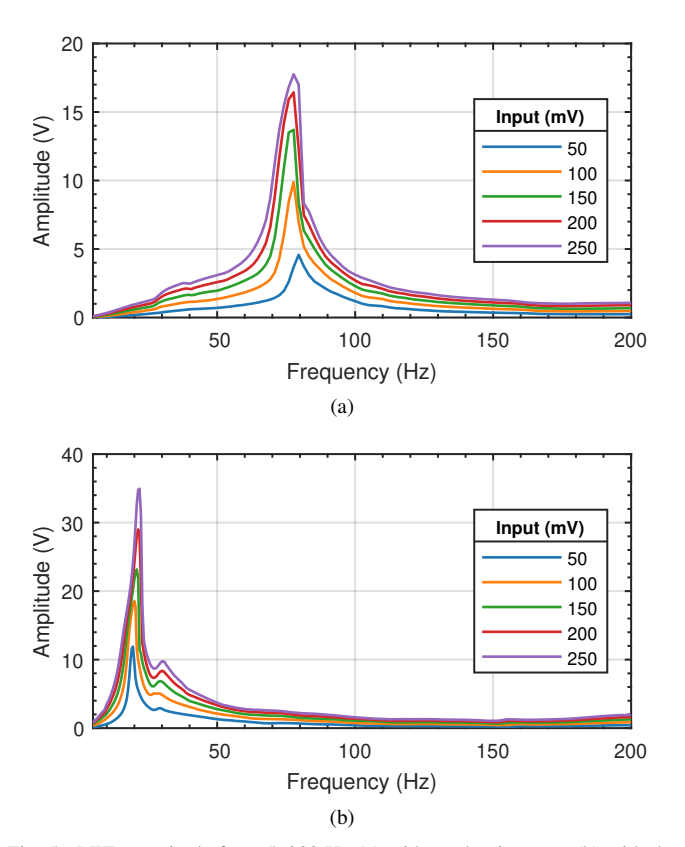
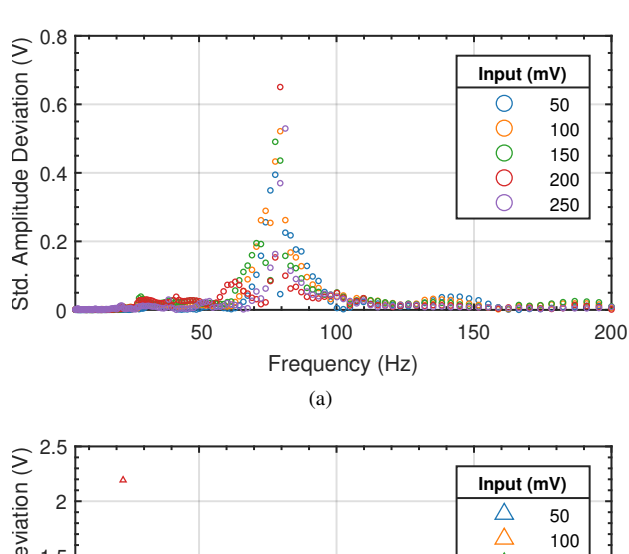


Fig. 5. PZT magnitude from 5–200 Hz (a) without the tip mass, (b) with the tip mass.

The standard magnitude deviation for the three sample sweeps in each PZT configuration with a majority of the points concentrated near zero indicates a consistent PZT response across the measured frequency range (Figs. 6(a) and 6(b)). The deviation is greatest around the resonant peaks and may benefit from a shaker setup with no loose probes or wires that could alter the system dynamics.

The PZT and accelerometer are approximately 180° out of phase at low frequencies (Figs. 7(a) and 7(b)), which corresponds to a delay related to the deflection time for the free end of the PZT cantilever to swing in the same direction as the fixed end mounted to the shaker. The absolute phase difference and corresponding delay decreases with frequency until after the resonant peak where the PZT and accelerometer are nearly in phase.



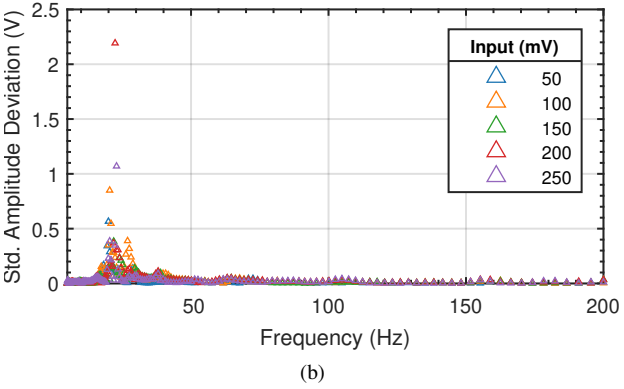


Fig. 6. PZT standard magnitude deviation from 5–200 Hz (a) without the tip mass, (b) with the tip mass.

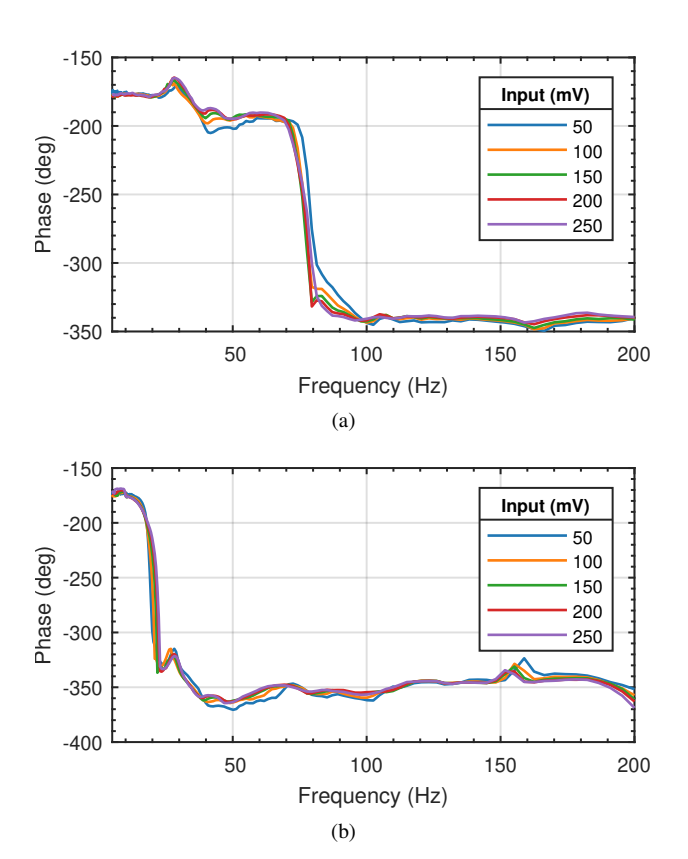


Fig. 7. PZT phase relative to the accelerometer from $5-200~{\rm Hz}$ (a) without the tip mass, (b) with the tip mass.

C. Machine Learning Model Predictions

The preprocessed measurement data, with 4830 total samples for each PZT configuration, was normalized and randomly split with 70% used for training and 30% used for testing. The models were trained with the training set and then evaluated with the testing set using the scikit-learn library in Python to determine the performance (Tables I and II).

TABLE I MODEL PERFORMANCE FOR THE PZT WITHOUT THE TIP MASS

Statistic	Stage 1			Stage 2
	MLP	Extra Trees	Support Vector	Extra Trees
MAE	0.1664	0.04884	0.3741	0.01760
MSE	0.08865	0.01417	0.4799	0.003353
\mathbb{R}^2	0.9881	0.9981	0.9357	0.9996

TABLE II
MODEL PERFORMANCE FOR THE PZT WITH THE TIP MASS

Statistic	Stage 1			Stage 2
	MLP	Extra Trees	Support Vector	Extra Trees
MAE	0.1997	0.03779	0.5018	0.01561
MSE	0.08717	0.007062	0.5437	0.002078
\mathbb{R}^2	0.9883	0.9991	0.9272	0.9997

The performance metrics considered are the mean absolute error (MAE), mean squared error (MSE), and coefficient of determination R². The second-stage model statistics show the overall ensemble model performance, and the higher R² score in the second stages indicates that the ensemble better fits the data compared to the individual first-stage models. Although a high R² score does not necessarily mean the model generalizes well to new data, the score suggests a consistent PZT response between the three sample sweeps. The PZT cantilever with the tip mass yields better accuracy compared to the PZT cantilever without, possibly due to the larger output dynamic range providing better separation between the samples. The MAE is only reduced by 11.3% from 0.01760 g to 0.01561 g, but the MSE is reduced by 38.0% from 0.003353 to 0.002078 by adding the tip mass, which indicates fewer prediction outliers and is confirmed visually by Figs. 8 and 9 showing the predicted acceleration and relative percent error for each prediction. The maximum absolute prediction error is reduced from 19% to 7% by adding the tip mass.

V. CONCLUSION AND FUTURE WORK

The PZT cantilever could be used simultaneously for energy harvesting and as a vibration sensor for predicting absolute acceleration with acceptable accuracy via machine learning. Predictions could include negative acceleration by considering the PZT voltage polarity in the model. Predictions could also be extended to the x-axis and y-axis or partial orientations with a multi-directional PZT system. Future work includes testing with multiple PZT cantilevers to study process and temperature variation effects on accuracy and to study the

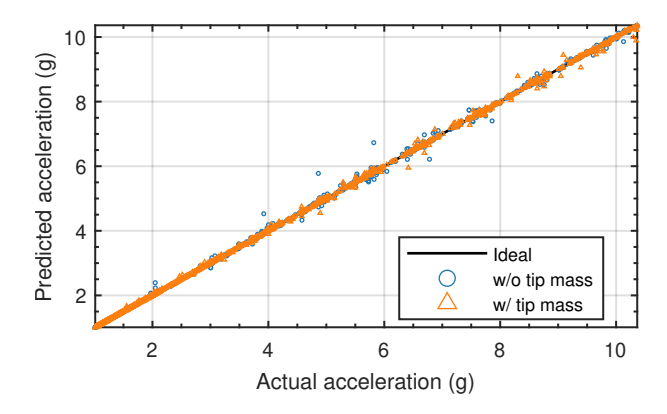


Fig. 8. Predicted vs. actual acceleration.

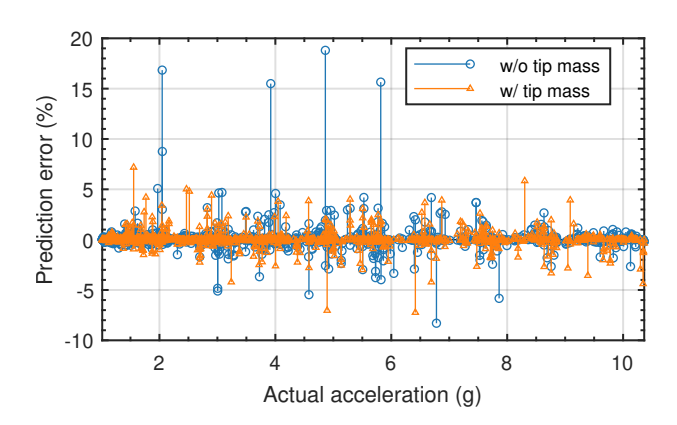


Fig. 9. Prediction error vs. actual acceleration.

model's generalizability with vibration inputs resembling realworld scenarios.

ACKNOWLEDGMENT

This research was supported by the Virginia Tech/Ford Alliance program. We appreciate Brian Robert with Ford Motors suggesting the idea of using PZT cantilevers for vibration sensing. This research was also supported in part by the National Science Foundation Award number 1814477.

REFERENCES

- S. J. Rupitsch, Piezoelectric Sensors and Actuators: Fundamentals and Applications, ser. Topics in Mining, Metallurgy and Materials Engineering. Berlin, Heidelberg: Springer, 2019.
- [2] S. Shi, W. Geng, K. Bi, Y. Shi, F. Li, J. He, and X. Chou, "High Sensitivity MEMS Accelerometer Using PZT-Based Four L-Shaped Beam Structure," *IEEE Sensors Journal*, vol. 22, no. 8, pp. 7627–7636, Apr. 2022.
- [3] C. Yang, B. Hu, L. Lu, Z. Wang, W. Liu, and C. Sun, "A Minia-turized Piezoelectric MEMS Accelerometer with Polygon Topological Cantilever Structure," *Micromachines*, vol. 13, no. 10, p. 1608, Oct. 2022.
- [4] S. Priya, H.-C. Song, Y. Zhou, R. Varghese, A. Chopra, S.-G. Kim, I. Kanno, L. Wu, D. S. Ha, J. Ryu, and R. G. Polcawich, "A Review on Piezoelectric Energy Harvesting: Materials, Methods, and Circuits," *Energy Harvesting and Systems*, vol. 4, no. 1, pp. 3–39, Jan. 2017.
- [5] L. Wu and D. S. Ha, "A Self-Powered Piezoelectric Energy Harvesting Circuit With an Optimal Flipping Time SSHI and Maximum Power Point Tracking," *IEEE Transactions on Circuits and Systems II: Express Briefs*, vol. 66, no. 10, pp. 1758–1762, Oct. 2019.

- [6] J. H. Hyun, N. Chen, and D. S. Ha, "Energy Harvesting Circuit for Road Speed Bumps Using a Piezoelectric Cantilever," in *IECON 2018* - 44th Annual Conference of the IEEE Industrial Electronics Society, Oct. 2018, pp. 4219–4223.
- [7] N. Chen, T. Wei, D. S. Ha, H. J. Jung, and S. Lee, "Alternating Resistive Impedance Matching for an Impact-Type Microwind Piezoelectric Energy Harvester," *IEEE Transactions on Industrial Electronics*, vol. 65, no. 9, pp. 7374–7382, Sep. 2018.
- [8] L. Wu, X.-D. Do, S.-G. Lee, and D. S. Ha, "A Self-Powered and Optimal SSHI Circuit Integrated With an Active Rectifier for Piezoelectric Energy Harvesting," *IEEE Transactions on Circuits and Systems I:* Regular Papers, vol. 64, no. 3, pp. 537–549, Mar. 2017.
- [9] T. Ruan, Z. J. Chew, and M. Zhu, "Energy-Aware Approaches for Energy Harvesting Powered Wireless Sensor Nodes," *IEEE Sensors Journal*, vol. 17, no. 7, pp. 2165–2173, Apr. 2017.
- [10] A. Kumar, A. Varghese, A. Sharma, M. Prasad, V. Janyani, R. P. Yadav, and K. Elgaid, "Recent development and futuristic applications of MEMS based piezoelectric microphones," *Sensors and Actuators A: Physical*, vol. 347, p. 113887, Nov. 2022.
- [11] H. Wang, M. Li, Y. Yu, Z. Chen, Y. Ding, H. Jiang, and H. Xie, "A Piezoelectric MEMS Loud Speaker Based on Ceramic PZT," in 2019 20th International Conference on Solid-State Sensors, Actuators and Microsystems & Eurosensors XXXIII (TRANSDUCERS & EUROSENSORS XXXIII), Jun. 2019, pp. 857–860.
- [12] M. Shirvanimoghaddam, K. Shirvanimoghaddam, M. M. Abolhasani, M. Farhangi, V. Zahiri Barsari, H. Liu, M. Dohler, and M. Naebe, "Towards a Green and Self-Powered Internet of Things Using Piezoelectric Energy Harvesting," *IEEE Access*, vol. 7, pp. 94533–94556, 2019.
- [13] A. Jain, J. Mao, and K. Mohiuddin, "Artificial neural networks: A tutorial," *Computer*, vol. 29, no. 3, pp. 31–44, Mar. 1996.
- [14] G. Biau and E. Scornet, "A random forest guided tour," *TEST*, vol. 25, no. 2, pp. 197–227, Jun. 2016.
- [15] A. J. Smola and B. Schölkopf, "A tutorial on support vector regression," Statistics and Computing, vol. 14, no. 3, pp. 199–222, Aug. 2004.